



SIZE EFFECT ON SHEAR STRENGTH OF NORMAL AND WIDE BEAMS SECTION. II ANALYTICAL STUDY

M Gamil ¹, Nabil A. B. Yehia ², and M. Salem ³

¹Assistant Lecturer, Reinforced concrete institute, Housing and Building National Research Center, Giza, Egypt

² Professor of RC structures, Faculty of Engineering, Cairo University, Giza, Egypt

³ Lecturer, Reinforced concrete institute, Housing and Building National Research Center, Giza, Egypt

ملخص البحث

مقاومة الكمرات الخرسانة المسلحة للقص والتي تقل بزيادة عمق الكمرات الفعال تسمى بتأثير الحجم. وفي بحث سابق أُجري برنامج عملي لدراسة هذه العوامل المؤثرة في مقاومة الكمرات الخرسانية في القص وتقييم المعادلة التي يتم بها حساب مقاومة الكمرات الخرسانية في القص في الكود المصري لتصميم وتنفيذ المنشآت الخرسانية. وفي هذا البحث وباستخدام برنامج "أباكوس 6.13" تم عمل نموذج عددي للكمرات التي اختبرت معمليا بغرض التحقق من دقة النموذج العددي في حساب مقاومة القص للكمرات وحيث ثبتت قدرة وكفاءة النموذج العددي في ذلك فقد امتد البحث لعمل دراسة بارامترية باستخدام نفس البرنامج التحليلي لتقدير قيم الحمل الأقصى للكمرات الخرسانية مع تغيير نسبة التسليح ، قوة ضغط الخرسانة، والعمق الفعال للكمرات الخرسانية.

ABSTRACT

The shear strength of reinforced concrete beams, which decreases with increase in depth, is prominently described as the size effect. The main objective of this research was to investigate to what extent the beam depth, width, longitudinal reinforcement ratio and concrete compressive strength, influence the ultimate shear capacity of reinforced concrete beams without transverse reinforcement. An experimental program was undertaken earlier ¹ to study these parameters and to evaluate the current Egyptian Code of practice (ECP 203-2017) ² empirical formula function for calculation shear strength of concrete beams.

The ultimate load was verified analytically using a finite element (FE) program "ABAQUS 6.13", and the results gave a good agreement with the experimental results. A parametric study was performed using the same FE program to estimate the ultimate load for beams and to compare the results among different variables; longitudinal steel ratio, concrete compressive strength, and the effective depth for beams.

Key Words: ABAQUS, size effect, concrete, shear strength.

INTRODUCTION

Shear problems usually vex structural engineers due to the absence of a unified theory that can explain different design situations where shear is involved.

Most of the design codes have adopted empirical methods with several different expressions that aim to express shear strength for concrete sections.

The current and the previous Egyptian Code of practice (ECP 203-2017)², (ECP 203-2007)³ depends on an empirical formula function only in concrete characteristic compressive strength for calculation of concrete shear strength in both normal and wide beams and do not even account for some basic and proven factors affecting the shear strength capacity of concrete members. Of these factors, the effect of member size and the percentage of longitudinal reinforcement on the shear capacity of beam elements.

The first aspect is concerned with the observation that under certain circumstances as the size of a reinforced concrete member increases the shear strength decreases. This so called "size effect" in shear.

The second aspect is concerned with the amount and distribution of longitudinal reinforcement in concrete members.

OUTLINE OF THE EXPERIMENTAL PROGRAM

M. Gamil¹ carried out an experimental program consists of eighteen beams with detailing as shown in Figure (1). Specimens were subjected to a three point bend test until failure. Detailed information of the specimens is summarized in Table 1.

Table 1: Details of the Specimens

Group	Beam Type	Nominal f_{cu} , N/mm ²	Specimen	Dimensions			Longitudinal reinforcement t	reinforcement ratio, %
				b, mm	t,mm	l_{eff} ,mm		
Group (I)	Wide Beams	25	B1	500	250	1350	7Y16	1.25
		25	B2	700	250	1350	10Y16	1.28
Group (II)		25	B3	700	150	750	10Y12	1.29
		25	B2	700	250	1350	10Y16	1.28
		25	B4	700	350	1950	14Y16	1.24
Group (III)	Normal Beams	25	B5	125	250	1350	3Y12	1.21
		25	B6	125	350	1950	2Y18	1.25
		25	B7	125	600	3368	2Y18+2Y16	1.30
Group (IV)	Wide Beams	25	B8	500	250	1350	8Y12	0.80
		25	B9	700	250	1350	11Y12	0.79
Group (V)		25	B10	700	150	750	9Y10	0.81
		25	B9	700	250	1350	11Y12	0.79
		25	B11	700	350	1950	9Y16	0.80
Group (VI)	Normal Beams	25	B12	125	250	1350	3Y10	0.84
		25	B13	125	350	1950	3Y12	0.83
		25	B14	125	600	3368	3Y16	0.84
Group (VII)	Wide Beams	87.5	B15	700	250	1350	10Y16	1.28
		87.5	B16	700	350	1950	14Y16	1.24
	Normal Beams	87.5	B17	125	250	1350	3Y12	1.21
		87.5	B18	125	600	3368	2Y18+2Y16	1.25

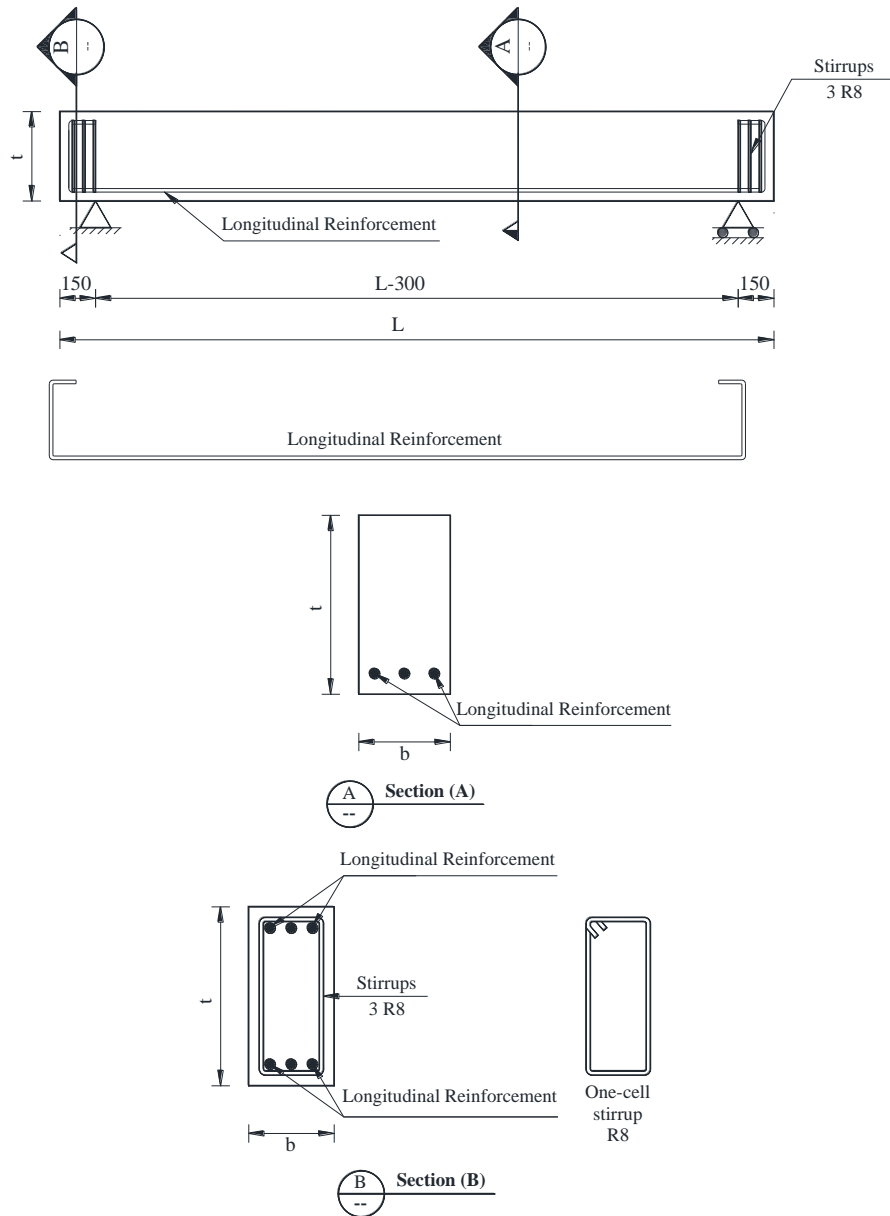


Figure 1: Details of specimens

FINITE ELEMENT MODELING

To study the behaviour of the beams, a numerical model includes the nonlinear behaviour of the constitutive materials; reinforcement bars, and concrete, separately was generated to investigate the ultimate capacity of the composite beams.

In order to reduce the computational time, only quarter of the beam was represented in the FE model taking into account the symmetry of the beams. The details of the reinforced concrete beam modelled in ABAQUS is shown in Figure (2).

In nonlinear analyses, each loading step is broken into increments so that the nonlinear solution path can be followed. ABAQUS/Standard automatically chooses the size of the subsequent increments. By the end of each increment, the structure is in (approximate) equilibrium. An iteration is an attempt to find an equilibrium solution in an increment. If

the model is not in equilibrium at the end of the iteration, ABAQUS/Standard tries another iteration. With every iteration the solution that ABAQUS/Standard obtains should be closer to equilibrium; however, sometimes the iteration process may diverge, subsequent iterations may move away from the equilibrium state. In that case, ABAQUS/Standard may terminate the iteration process and attempt to find a solution with a smaller increment size.

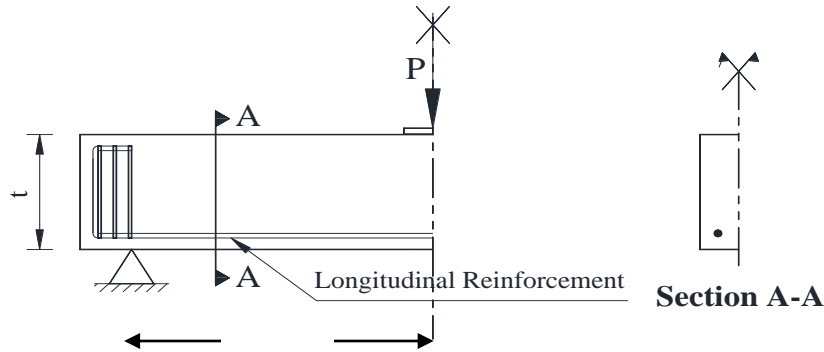


Figure 1: Simplified Beam Details used in the FE Model

THE MATERIAL MODELS

Concrete model

ABAQUS 6.13 program provides the capability of simulating the damage using either of the three crack models for reinforced concrete elements:

1. Smearred crack concrete model.
2. Brittle crack concrete model
- 3 Concrete damaged plasticity model.

Out of the three concrete crack models, the concrete damaged plasticity model is selected in the present study as this technique has the potential to represent complete inelastic behaviour of concrete both in tension and compression including damage characteristics, B. L. Wahalathantri et al ⁴.

The concrete damaged plasticity model assumes that the two main failure mechanisms in concrete are the tensile cracking and the compressive crushing. In this model, the uniaxial tensile and compressive behaviour is characterized by damaged plasticity. Both of these phenomena are the result of micro-cracking. The evolution of the yield (or failure) surface is determined by two hardening variables, $\tilde{\epsilon}_t^{pl}$ and $\tilde{\epsilon}_c^{pl}$, where $\tilde{\epsilon}_t^{pl}$ and $\tilde{\epsilon}_c^{pl}$ are the tension and compression equivalent plastic strains, respectively. Each of them is linked to degradation mechanisms under tensile or compressive stress conditions, as shown in Figure 2). The degradation of the elastic stiffness is characterized by two damage variables, d_t and d_c .

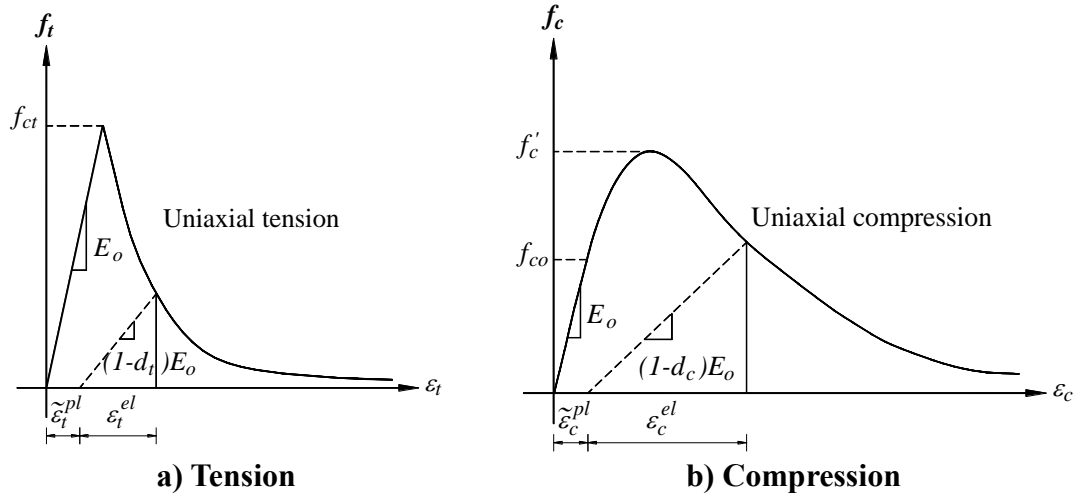


Figure 2: Response of Concrete to Uniaxial Loading in A) Tension B) Compression (ABAQUS Analysis User's Manual⁵)

Tension stiffening relationship

A. Hillerborg, et al.⁶ suggested a linear softening curve for concrete tension behavior, as shown in Figure 3(a), and proposed a crack width, w_c , of 0.01~0.02mm based on experiments. The CEB-FIP Model Code⁷ proposed a bilinear stress-crack opening relationship for cracked concrete subjected to tension as given in Equations (1) and (2), Figure 3(b).

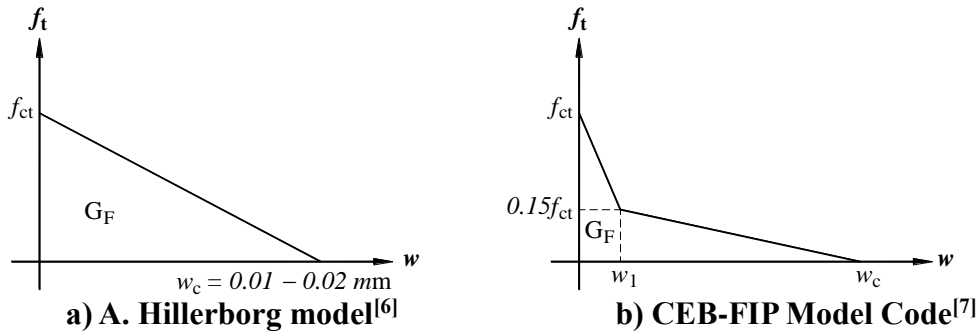


Figure 3: Concrete Tension Stiffening Models

$$f_t = \frac{0.15f_{ct}}{w_c - w_1} (w_c - w) \quad \text{for } 0 \leq f_t \leq 0.15f_{ct} \quad (1)$$

$$f_t = f_{ct} \left(1 - 0.85 \frac{w}{w_1} \right) \quad \text{for } 0.15f_{ct} \leq f_t \leq f_{ct} \quad (2)$$

$$w_1 = 2 \frac{G_F}{f_{ct}} - 0.15w_c \quad (3)$$

$$w_c = \alpha_F \frac{G_F}{f_{ct}} \quad (4)$$

Where f_{ct} is the tensile strength of concrete (MPa), f_t is the tensile stress, w is the crack opening (mm), w_1 is the crack opening (mm) for $f_t = 0.15f_{ct}$, w_c is the crack opening (mm) for $f_t = 0$, G_F is the fracture energy (Nmm/mm^2), and α_F is a coefficient which

depends on maximum aggregate size, d_{max} (mm). $\alpha_F = 8, 7,$ and 5 for d_{max} (mm) = $8, 16,$ and 32 respectively, as proposed by CEB-FIP Model Code⁶. Concrete in tension was modeled as linear elastic brittle material with strain softening. Tension stiffening is allowed by modifying the concrete softening behavior. Post-cracking stress-strain relationship was as suggested by B. Massicotte, A.E. Elwi, J.G. MacGregor⁸. and is shown in Figure (5). This relationship assumed that the strain softening after cracking reduces the stress to zero at a total strain of about 16 times the strain at first cracking. The curve, suggested by Massicotte⁷, was softened to permit a relatively gradual response behavior and consequently to decrease the convergence problems, as shown in Figure (6) as suggested by Said M. Allam⁹.

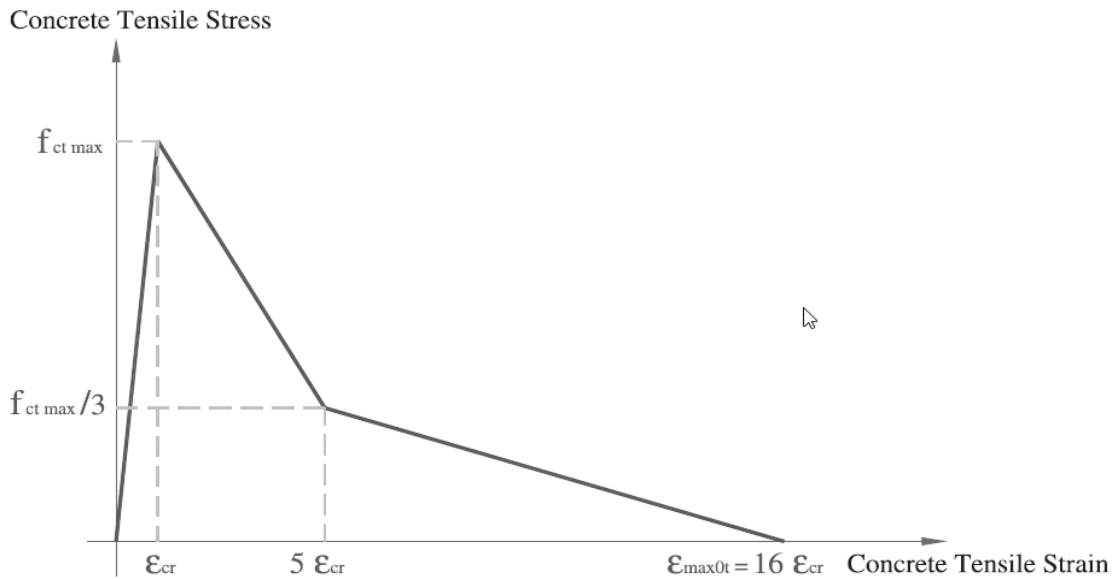


Figure Error! No text of specified style in document. : Tension softening curve suggested by Massicotte et al.⁸.

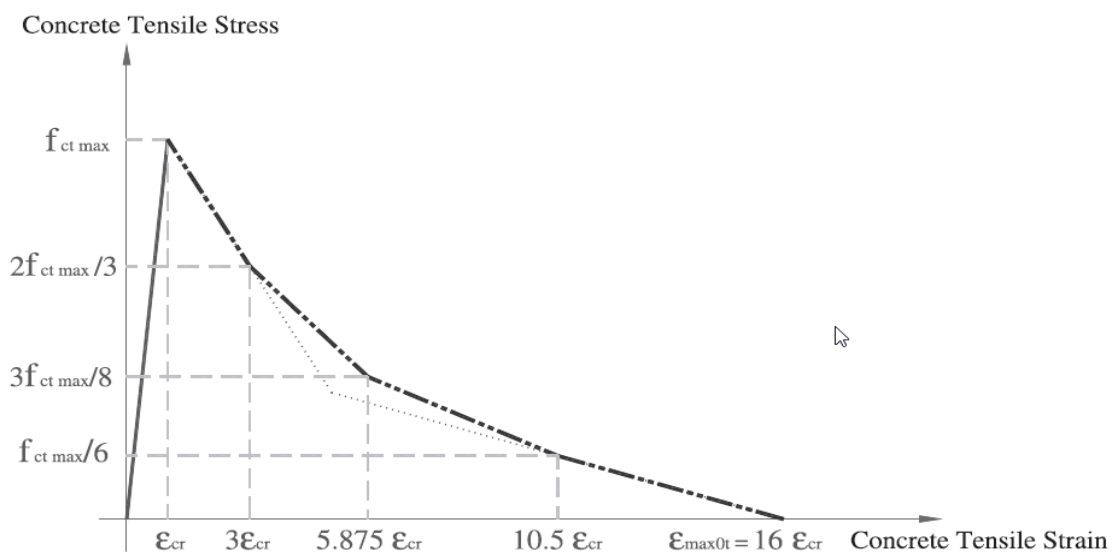


Figure 6: Modified tension softening curve⁹

Compressive stress-strain relationship

In this paper, the uniaxial nonlinear stress-strain relationship proposed by L. P. Saenz¹⁰, was used as a basic stress-strain curve, and linear behavior was assumed up to $f_{co} = 0.4f'_c$, as proposed in the Eurocode 2 (ENV 1992-1-1:1992)¹¹. Where, f'_c is the compressive cylinder strength of concrete.

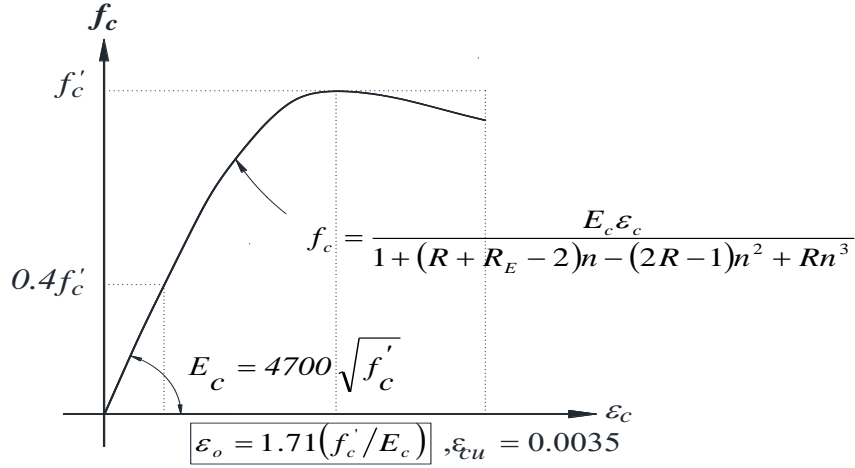


Figure 7: Stress-Strain Behavior of Concrete under Uniaxial Compression

The Poisson's ratio ($\nu_c = 0.2$ is recommended in this study) controls the volume changes of concrete for stresses below the critical stress level, f_{co} (in the elastic region). For non-linear analysis, the stress-strain relation for concrete in compression recommended by L. P. Saenz¹⁰, Figure), is defined by the following form:

$$f_c = \frac{E_c \varepsilon_c}{1 + (R + R_E - 2) \left(\frac{\varepsilon_c}{\varepsilon_o}\right) - (2R - 1) \left(\frac{\varepsilon_c}{\varepsilon_o}\right)^2 + R \left(\frac{\varepsilon_c}{\varepsilon_o}\right)^3} \quad (5)$$

Where E_c is the elastic modulus of concrete which is calculated according to the ACI 318-14¹² as follows:

$$E_c = 4700\sqrt{f'_c} \quad (6)$$

And ε_o is calculated according to the following equation proposed by Salem¹³:

$$\varepsilon_o = 1.71 \frac{f'_c}{E_c} \quad (7)$$

Where E_o and R_E are as follows:

$$E_o = \frac{f'_c}{\varepsilon_o} \quad (8)$$

$$R_E = \frac{E_c}{E_o} \quad (9)$$

And R was calculated according to the following equation:

$$R = \frac{R_E(R_\sigma - 1)}{(R_\varepsilon - 1)^2} - \frac{1}{R_\varepsilon} \quad (1)$$

Where $R_\varepsilon = R_\sigma = 4$ as reported by M. M. A. Salem¹³.

$$R = \frac{4R_E - 3}{12} \quad (2)$$

Steel reinforcing bar model

The constitutive behaviour of steel is predicted using an elastic perfectly plastic model, as described in (ABAQUS 6.13)⁵. In this approach, the steel behaviour is elastic up to the yield stress. At this point, the material yields under constant load, as shown in Figure (8). The parameters required by this formulation are the modulus of elasticity ($E_s = 200$ GPa), poisson's ratio ($\nu_s = 0.3$), and the yield stress ($f_{sy} = 400$ MPa).

The steel reinforcement was embedded to the concrete assuming that there is a perfect bond between the concrete and the steel reinforcement. Figure (9) show modelled beam in ABAQUS.

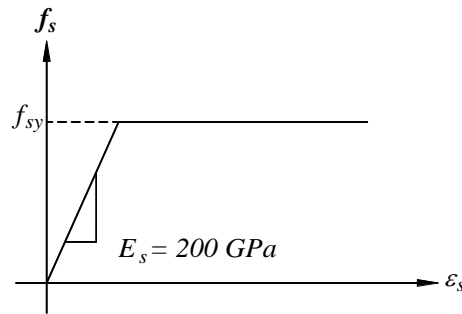


Figure 8: Stress-Strain Relationship for Steel Reinforcement

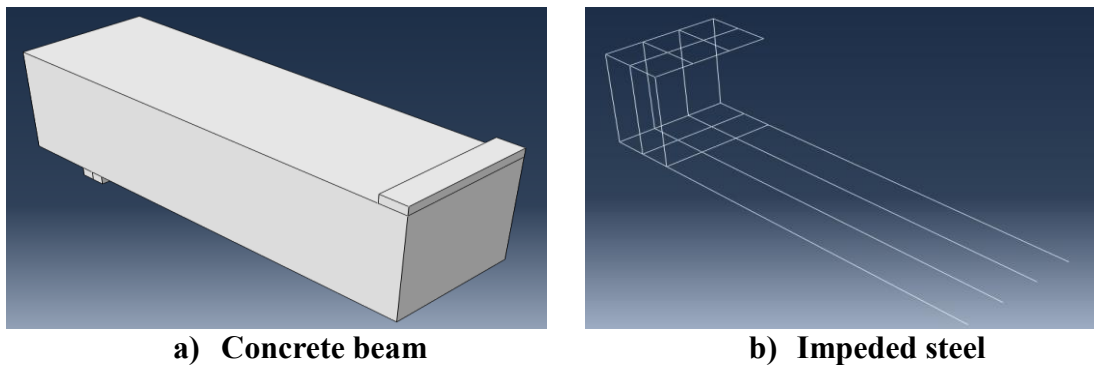


Figure 9: Beam Model in Abaqus

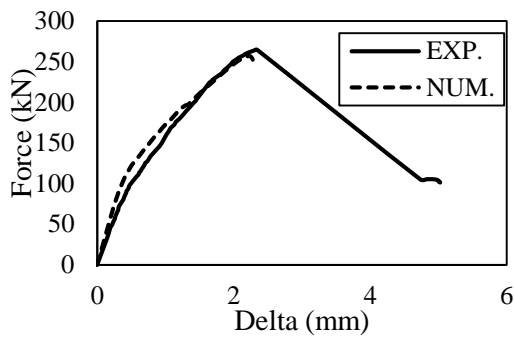
NONLINEAR ANALYSIS AND PARAMETRIC STUDY

NUMERICAL MODEL VERIFICATION

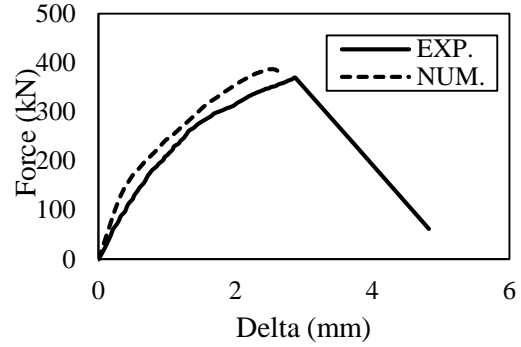
The developed finite element (FE) model was used to validate the results of the experimental data performed by M. Gamil¹. The load-deflection curves of the beams were first verified to check for the validity of the concrete and steel curves that were inserted in the FE model. Also, this verification was performed to check for the ultimate capacity that could be estimated using the FE model.

Verification of the load-deflection behavior

The experimental load-deflection curves of beams are hereby plotted versus the load-deflection curves estimated using the finite element model, as shown in Figure (10) to Figure (16). A comparison between the ultimate loads from numerical model and the ultimate loads from tests is shown in Table 2. It was concluded that the finite element model gives a reliable load-deflection relationship for the reinforced concrete beams.

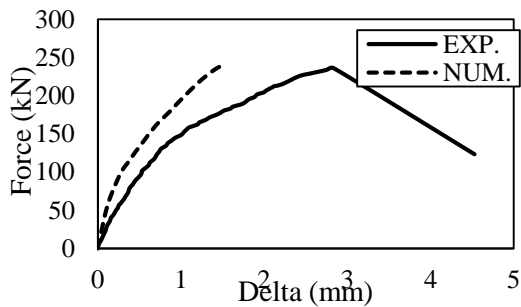


a) B1

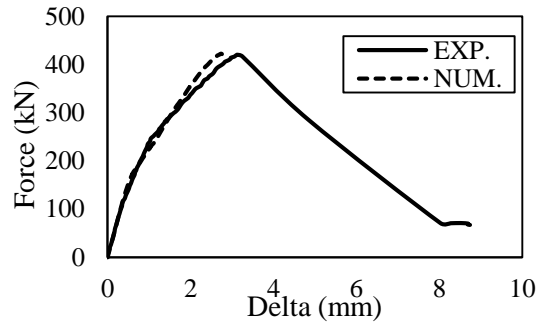


b) B2

Figure 10 : Experimental Versus Numerical results for the load-deflection of specimens in group I.

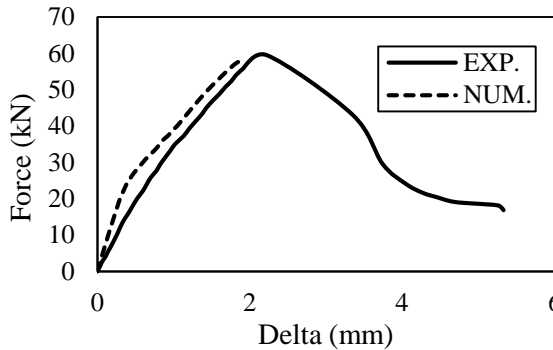


a) B3

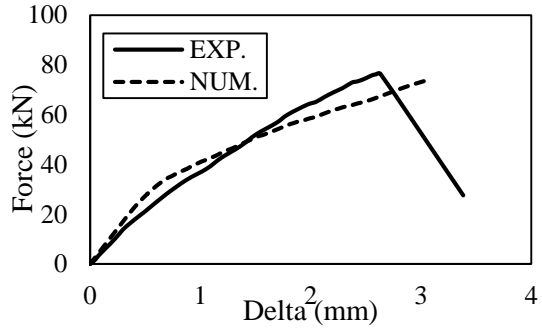


b) B4

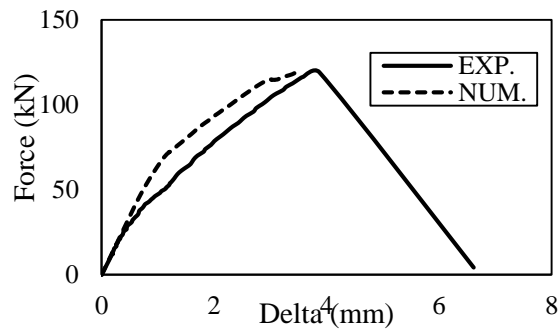
Figure 11 : Experimental Versus Numerical results for the load-deflection of specimens in group II.



a) B5

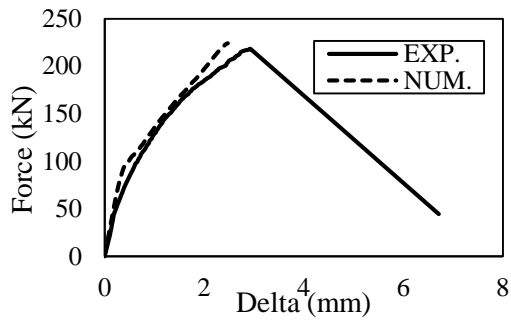


b) B6

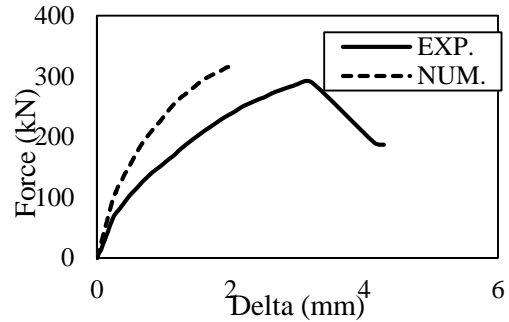


c) B7

Figure 12 : Experimental Versus Numerical results for the load-deflection of specimens in group III.

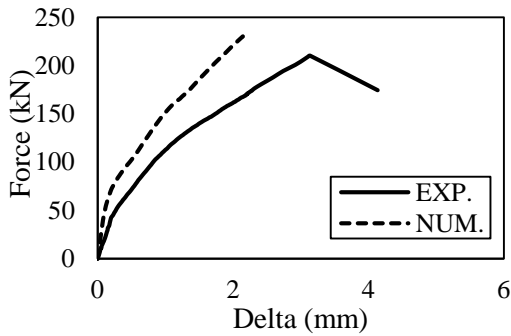


a) B8

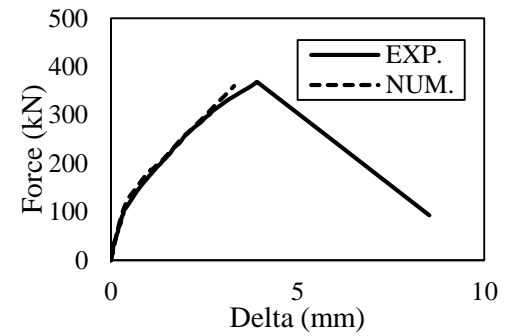


b) B9

Figure 13 : Experimental Versus Numerical results for the load-deflection of specimens in group IV.

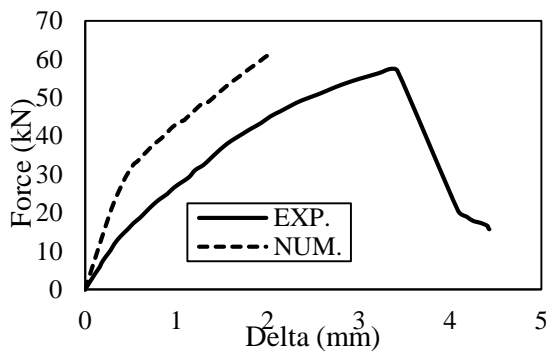


a) B10

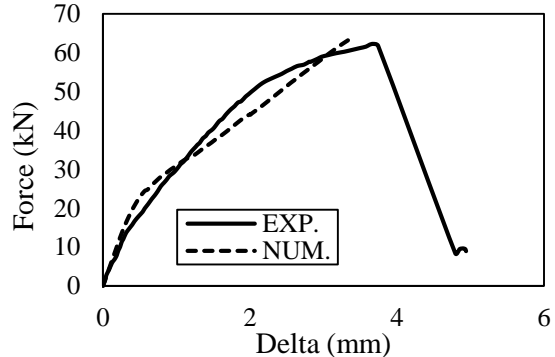


b) B11

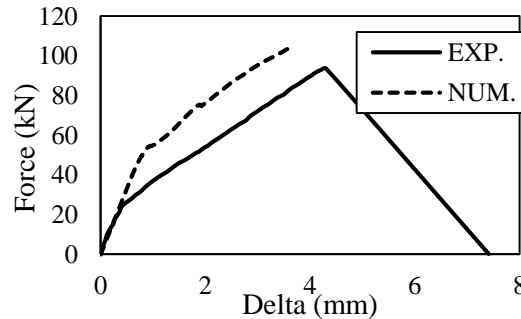
Figure 14 : Experimental Versus Numerical results for the load-deflection of specimens in group V.



a) B12



b) B13



c) B14

Figure 15 : Experimental Versus Numerical results for the load-deflection of specimens in group VI.

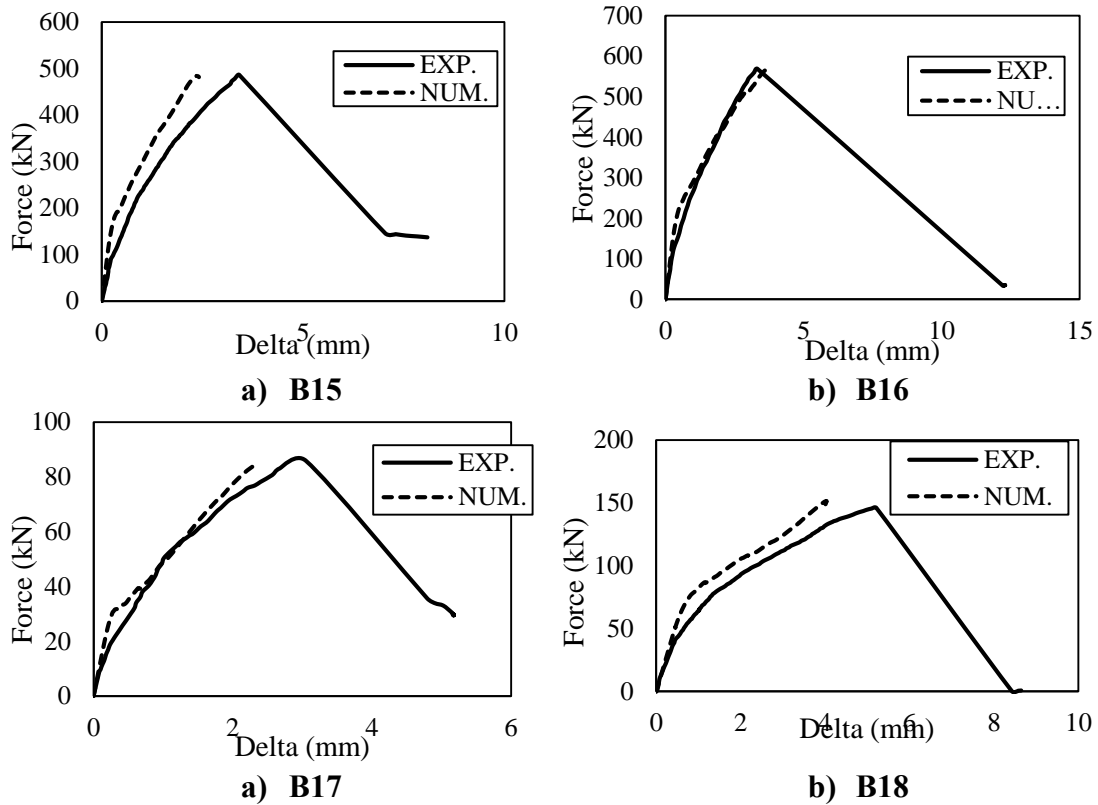


Figure 16 : Experimental Versus Numerical results for the load-deflection of specimens in group VII.

Table 2: Numerical vs. Experimental shear capacity

Group	Specimen	P_{test} , KN	P_{Num} , KN	Difference= $(Num-test)/ test$ (%)
Group (I)	B1	264.6	256.9	-2.910
	B2	369.4	387.4	4.873
Group (II)	B3	236.3	238.6	0.973
	B2	369.4	387.4	4.873
	B4	420.2	422.4	0.524
Group (III)	B5	59.4	58.1	-2.189
	B6	76.4	73.5	-3.796
	B7	119.1	118.8	-0.252
Group (IV)	B8	218.4	224.2	2.656
	B9	289.6	315.3	8.874
Group (V)	B10	210.1	230.4	9.662
	B9	289.6	315.3	8.874
	B11	368.3	360.1	-2.226
Group (VI)	B12	57.4	61.7	7.491
	B13	62.2	63.4	1.929
	B14	93.4	104.0	11.349
Group (VII)	B15	486.1	483.7	-0.494
	B16	569.4	565.2	-0.738
	B17	85.9	85.2	-0.815
	B18	146.1	151.6	3.765

PARAMETRIC STUDY

The calibrated finite element model discussed above was used to predict the ultimate load of different beams. The parametric study in this paper was performed on the two grades of concrete, which were used in the experimental study; 25 MPa and 87.5 MPa. Table 3 shows specimen details of parametric study. The normalized shear stress for the specimens in parametric study is shown in Table 3.

Table 2: Details of Specimens in Parametric Study

Group	Specimen	Dimensions, mm			Longitudinal reinforcement	reinforcement ratio, %	f_{cu} (N/mm ²)
		b	t	l_{eff}			
G1	B19	500	900	5250	7Y32	1.28	25
	B20	500	1250	7350	7Y37	1.23	25
	B21	500	1500	8850	7Y41	1.25	25
	B22	500	1750	10350	7Y44	1.23	25
	B23	500	2000	11850	7Y47	1.23	25
	B24	500	2250	13350	7Y50	1.23	25
	B25	500	2500	14850	7Y52	1.20	25
	B26	500	2750	16350	7Y55	1.22	25
	B27	500	3000	17850	7Y58	1.24	25
G2	B28	500	900	5250	7Y25	0.78	25
	B29	500	1250	7350	7Y30	0.81	25
	B30	500	1500	8850	7Y33	0.81	25
	B31	500	1750	10350	7Y36	0.82	25
	B32	500	2000	11850	7Y38	0.80	25
	B33	500	2250	13350	7Y40	0.79	25
	B34	500	2500	14850	7Y43	0.82	25
	B35	500	2750	16350	7Y45	0.82	25
	B36	500	3000	17850	7Y47	0.81	25
G3	B37	500	900	5250	7Y32	1.28	87.5
	B38	500	1250	7350	7Y37	1.23	87.5
	B39	500	1500	8850	7Y41	1.25	87.5
	B40	500	1750	10350	7Y44	1.23	87.5
	B41	500	2000	11850	7Y47	1.23	87.5
	B42	500	2250	13350	7Y50	1.23	87.5
	B43	500	2500	14850	7Y52	1.20	87.5
	B44	500	2750	16350	7Y55	1.22	87.5
	B45	500	3000	17850	7Y58	1.24	87.5
G4	B46	500	900	5250	7Y25	0.78	87.5
	B47	500	1250	7350	7Y30	0.81	87.5
	B48	500	1500	8850	7Y33	0.81	87.5
	B49	500	1750	10350	7Y36	0.82	87.5
	B50	500	2000	11850	7Y38	0.80	87.5
	B51	500	2250	13350	7Y40	0.79	87.5
	B52	500	2500	14850	7Y43	0.82	87.5
	B53	500	2750	16350	7Y45	0.82	87.5
	B54	500	3000	17850	7Y47	0.81	87.5

Table 3: Normalized Shear Strength for specimens in parametric study

Group	Specimen	P _{num} , KN	Q _{num} , KN	f _{cu} , N/mm ²	q _{num} , N/mm ²	q _{num} /(f _{cu}) ^{0.5} (N) ^{1/2} /mm
G1	B19	650.83	325.42	25	0.744	0.149
	B20	740.64	370.32	25	0.605	0.121
	B21	813.13	406.57	25	0.551	0.110
	B22	882.06	441.03	25	0.511	0.102
	B23	970.71	485.36	25	0.492	0.098
	B24	1067.20	533.62	25	0.480	0.096
	B25	1159.60	579.80	25	0.469	0.094
	B26	1252.50	626.25	25	0.460	0.092
	B27	1342.70	671.33	25	0.451	0.090
G2	B28	568.26	284.13	25	0.649	0.130
	B29	627.56	313.78	25	0.512	0.102
	B30	685.13	342.56	25	0.464	0.093
	B31	740.93	370.47	25	0.430	0.086
	B32	813.24	406.62	25	0.412	0.082
	B33	890.78	445.39	25	0.400	0.080
	B34	973.01	486.50	25	0.393	0.079
	B35	1038.60	519.28	25	0.381	0.076
	B36	1119.50	559.73	25	0.376	0.075
G3	B37	845.46	422.73	87.5	0.966	0.103
	B38	954.77	477.39	87.5	0.779	0.083
	B39	1052.05	526.03	87.5	0.713	0.076
	B40	1143.10	571.55	87.5	0.663	0.071
	B41	1234.16	617.08	87.5	0.625	0.067
	B42	1328.00	664.00	87.5	0.597	0.064
	B43	1434.79	717.39	87.5	0.580	0.062
	B44	1551.31	775.66	87.5	0.569	0.061
	B45	1651.18	825.59	87.5	0.555	0.059
G4	B46	648.52	324.26	87.5	0.741	0.079
	B47	722.48	361.24	87.5	0.590	0.063
	B48	811.57	405.78	87.5	0.550	0.059
	B49	899.92	449.96	87.5	0.522	0.056
	B50	980.43	490.21	87.5	0.496	0.053
	B51	1064.40	532.20	87.5	0.478	0.051
	B52	1142.46	571.23	87.5	0.462	0.049
	B53	1224.33	612.17	87.5	0.449	0.048
	B54	1316.70	658.35	87.5	0.443	0.047

The numerical results of the parametric study specimens showed that as the beam depth increase the shear strength of the beam decrease. Figure (17) to Figure (20) shows the normalized shear strength for numerical model and the normalized codes predicting shear strength versus depth/width in-groups G1, G2, G3, and G4.

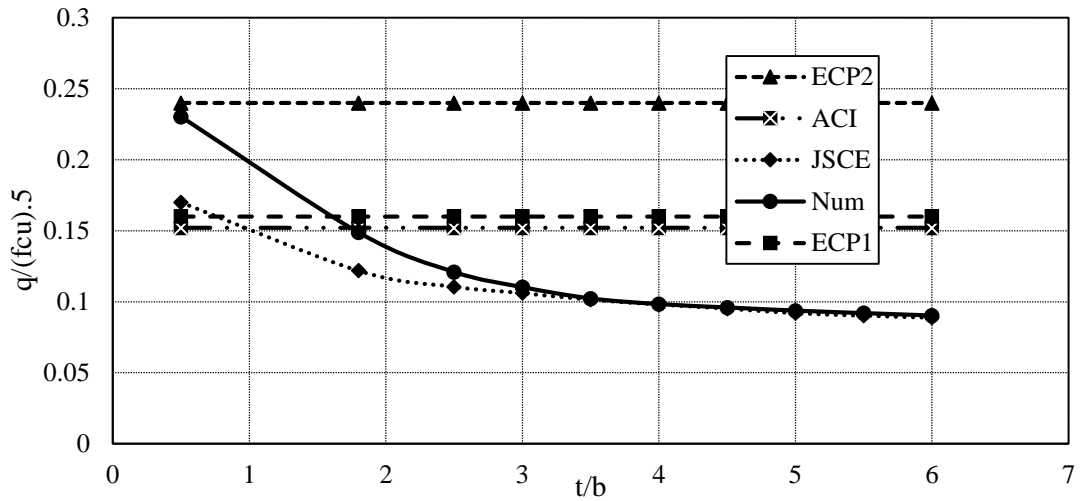


Figure 17: Normalized shear stress vs. depth/width ratio for specimens in G1

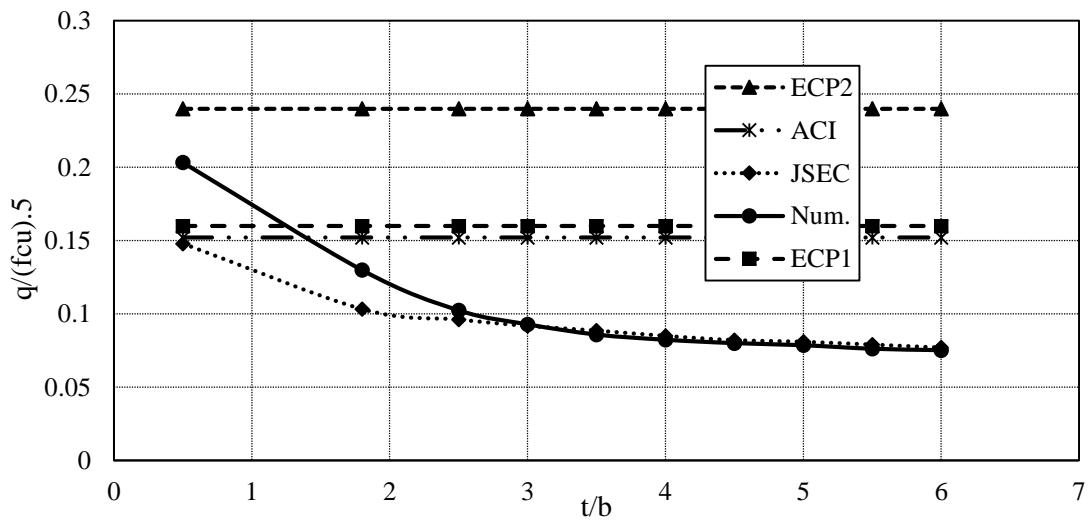


Figure 18: Normalized shear stress vs. depth/width ratio for specimens in G2

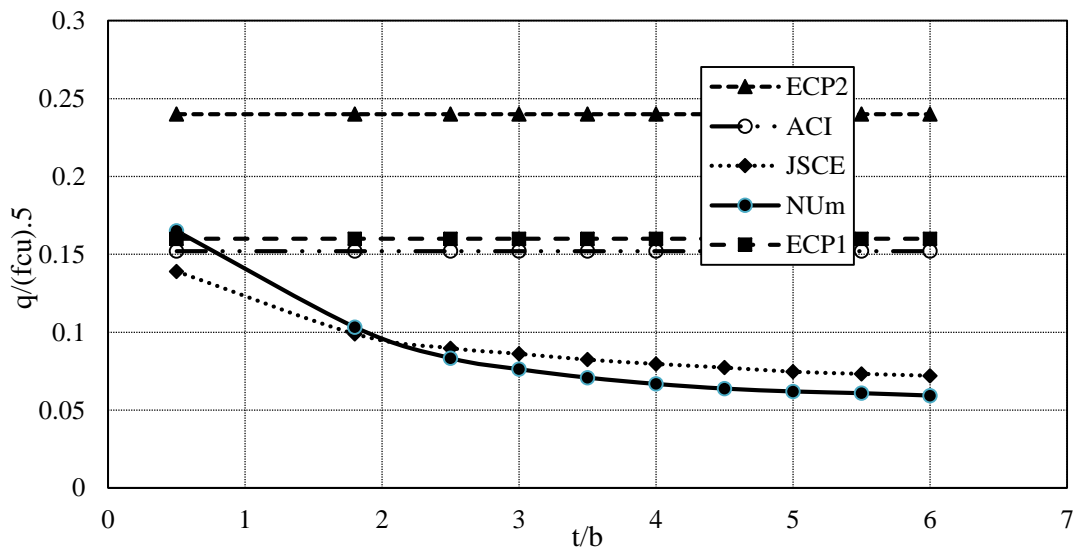


Figure 19: Normalized shear stress vs. depth/width ratio for specimens in G3

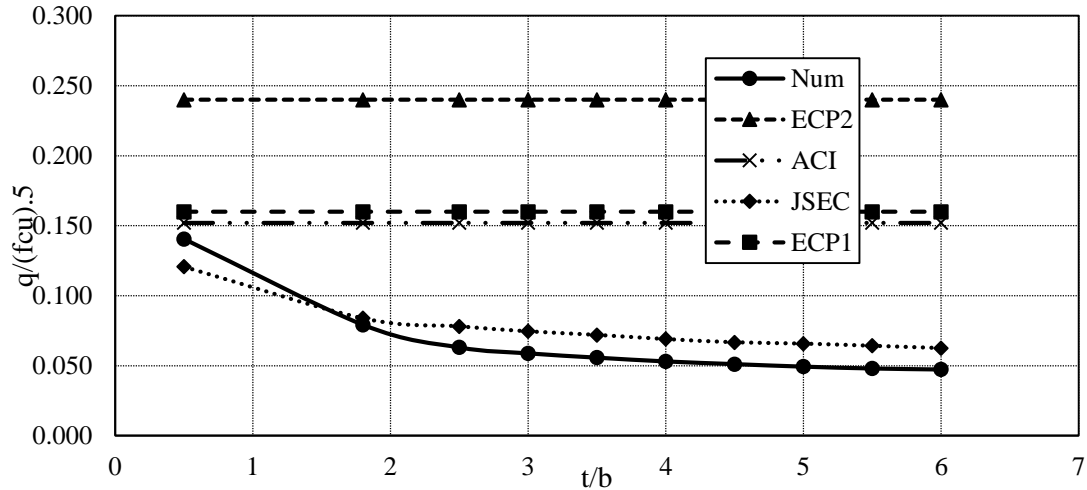


Figure 20: Normalized shear stress vs. depth/width ratio for specimens in G4

Curve fitting Figure (17) to (20), yields the following equations:

$$y = 3 * 10^{-8}x^2 - .0001x + 0.2575 \text{ for } G1 \text{ with } R^2=0.9829 \quad (12)$$

$$y = 3 * 10^{-8}x^2 - .0001x + 0.2287 \text{ for } G2 \text{ with } R^2=0.9832 \quad (13)$$

$$y = 2 * 10^{-8}x^2 - .0001x + 0.1845 \text{ for } G3 \text{ with } R^2=0.9821 \quad (14)$$

$$y = 2 * 10^{-8}x^2 - .00009x + 0.1554 \text{ for } G4 \text{ with } R^2=0.961 \quad (15)$$

The first term in the equations can be represented by factor α where $\alpha = 1$ in N.S.C. $f_{cu}=25$ Mpa , $\alpha = 2/3$ in H.S.C. $f_{cu}=87.5$ Mpa. The second term is almost constant. By trial and error, the third term is found equal $0.24\alpha^3\sqrt{\rho}$.

The following equation was derived:

$$q = S\sqrt{f_{cu}} \quad (3)$$

Where:

$$S = (3*10^{-8}) \alpha^2 t^2 - (1*10^{-4}) t + 0.24\alpha^3\sqrt{\rho}$$

$$\alpha = 1 \quad f_{cu}=25 \text{ Mpa}$$

$$= (2/3) \quad f_{cu}=87.5 \text{ Mpa}$$

t beam depth

$$\rho \text{ longitudinal reinforcement ratio} = \frac{A_s}{bd}$$

CONCLUSIONS

The results of the numerical analysis could be summarized as follows:

The analytical models gave good agreement with the experimental results.

For the same longitudinal reinforcement ratio, and for the same (shear span/effective length) ratio, and the same compressive strength of concrete, increasing the effective depth, decreases the shear strength.

As the longitudinal reinforcement ratio increase the shear strength increase.

As the concrete compressive strength increase the shear strength increase.

The decreasing rate of shear strength decreases as the effective depth increase.

The longitudinal reinforcement ratio and the depth should be taken into consideration in shear strength code formula to give a safe and convenient design for shear.

REFERENCES

1. M. Gamil "Size Effect on Shear Strength of Normal and Wide Beams," PhD Thesis, Cairo University, Egypt, Under way.
2. Egyptian Code of Practice for Design and Construction of Reinforced Concrete Buildings, 2017.
3. Egyptian Code of Practice for Design and Construction of Reinforced Concrete Buildings, 2007.
4. B. L. Wahalathantri, D. P. Thambiratnam, T. T. Chan and S. Fawzia, "A Material Model for Flexural Crack Simulation in Reinforced Concrete Elements using ABAQUS," in The First International Conference on Engineering, Designing and Developing the Built Environment for Sustainable Wellbeing, Queensland University of Technology, Queensland University of Technology, Brisbane, Qld, pp. 260-264, 2011.
5. ABAQUS Analysis User's Manual.
6. A. Hillerborg, M. Modeer and P.-E. Petersson, "Analysis of Crack Formation and Crack Growth in Concrete by Means of Fracture Mechanics and Finite Elements," *Cement and Concrete Research*, vol. 6, no. 6, pp. 773-781, November 1976.
7. Comite Euro - International Du Beton (CEB-FIP Model Code), 1990.
8. B. Massicotte, A.E. Elwi, and J. G. MacGregor "Tension stiffening model for planar reinforced concrete members," *ASCE Journal of Structural Engineering*, vol. 16, 1990.
9. Said M. Allam , Mohie S. Shoukry, Gehad E. Rashad, Amal S. Hassan "Evaluation of tension stiffening effect on the crack width calculation of flexural RC members," *Alexandria Engineering Journal*, 2013
10. L. P. Saenz, "Discussion of Paper By P. Desai, S. Krishnan; Equation for the Stress-Strain Curve of Concrete," *Journal of the American Concrete Institute*, Proc. No. 9, 1964, pp. 1229-1235.
11. Eurocode 2: Design of Concrete Structures - Part 1: General Rules and Rules for Buildings (ENV 1992-1-1:1992).
12. Building Code Requirements for Structural Concrete (ACI 318-14).
13. Salem, Mohamed Morsy Abdel-Ghaffar, "Flexural and Long-Term Behavior of CFRP-Strengthened Reinforced Concrete Beams," PhD Thesis, Hannover, Germany, 2012